

CHANDRA observation of the narrow-line Seyfert 1 galaxy IRAS 13224-3809

F. Pfefferkorn, Th. Boller, V. Burwitz and P. Predehl

Max-Planck-Institute for Extraterrestrial Physics, Giessenbachstr., 85748 Garching, Germany

E-mail(FP): pfefferk@mpe.mpg.de

ABSTRACT

The narrow-line Seyfert 1 galaxy (NLS1) IRAS 13224-3809 has been observed with the *CHANDRA* High Resolution Camera (HRC-I) for 12 ksec on February, 2, 2000. The source was proposed for *CHANDRA* observations to precisely determine the X-ray centroid position and to investigate the timing properties of the most X-ray variable Seyfert galaxy. The position derived from *CHANDRA* confirms that the X-ray emission is associated with IRAS 13224-3809. The *CHANDRA* HRC-I light curve shows indications for a possible presence of a quasi-periodic oscillation. The strongest signal is found at 2500 sec. Accretion disk instabilities may provide a plausible explanation for the quasi-periodic oscillations.

KEY WORDS: galaxies: active — galaxies: individual: IRAS 13224-3809 — galaxies: Seyfert — X-rays: galaxies

1. Introduction

The narrow-line Seyfert 1 galaxy (NLS1) IRAS 13224-3809 was the first galaxy proposed for monitoring observations with the *ROSAT* High Resolution Imager (HRI) (Boller et al., 1997). The most important observational fact is the detection of multiple strong flaring events during the 30 day observations. The authors found five giant-amplitude variations with the most extreme variability of a factor of 57 in 2 days. In addition, other *ROSAT* observations were performed, mostly with the HRI detector during 1992 and 1998. To measure the precise X-ray position, IRAS 13224-3809 has been proposed for an observation with the *CHANDRA* satellite.

2. Data reduction

IRAS 13224-3809 has been observed with the Chandra High Resolution Camera (HRC-I) on February, 2, 2000 between 15:16:28.59 UT and 18:41:04.25 UT with an effective exposure time of 12271.6 sec.

Inspection of the image with the source constructed from the reprocessed level 2 photon event file (`hrcf00328N002_evt2.fits`) indicates that the aspect reconstruction was not yet perfect as the FWHM of the source is ~ 1.04 arcsec which is larger than that expected from the instrument. A detailed analysis revealed that the source moved around the mean source position by approximately ± 0.5 arcsec with the dither period. This analysis was performed by computing the centroid in x ,

y , t for 100 consecutive events that lie within a circle of 2 arcsec around the mean source position. This 100 event window is shifted always by one event giving a smooth curve which shows the displacement of the centroid versus time giving us a correction vector. This vector is then used to correct the position of the individual photon events. The data reduction, correction, and extraction was performed using routines written in IDL. Using the correction vector we obtain a more realistic FWHM of ~ 0.64 arcsec for IRAS 13224-3809. This value is still larger than the expected value for the instrument indicating that extended X-ray emission is present around IRAS 13224-3809. A maximum likelihood source detection using `CELLDETECT` (from the CIAO data analysis package) performed on the binned image also indicates that the source FWHM is greater than that of the instrumental PSF (PSF-ratio=1.43187).

After checking the radial profile of the source we chose an extraction radius of 9 arcsec around the source so that also the photons from the diffuse emission could be collected. The background selection was performed by selecting photons in 8 regions, each with a radius of 9 arcsec. The regions are located 20 arcsec from the source.

During the observation the total number of events, especially all background, rose by a factor $\sim 3-4$ over a time span of ~ 2000 sec. Higher than normal solar activity is the most probable cause for this increase, which leads to a leakage of source counts based on the dead-time of the instrument. The ratio of detected to lost

photons versus time is given in deadtime correction file. This file was then used to correct lower count rate of the source during times with high background count rates. Only the photons lying in the goodtime intervals were used.

3. The *CHANDRA* position of IRAS 13224–3809

With the *CHANDRA* satellite one can determine the position of the X-ray emission with an unprecedented precision. In Fig. 1, we show an optical image taken from the Palomar Digitized Sky Survey (DSS) overlaid with a *CHANDRA* X-ray contour map of IRAS 13224–3809.

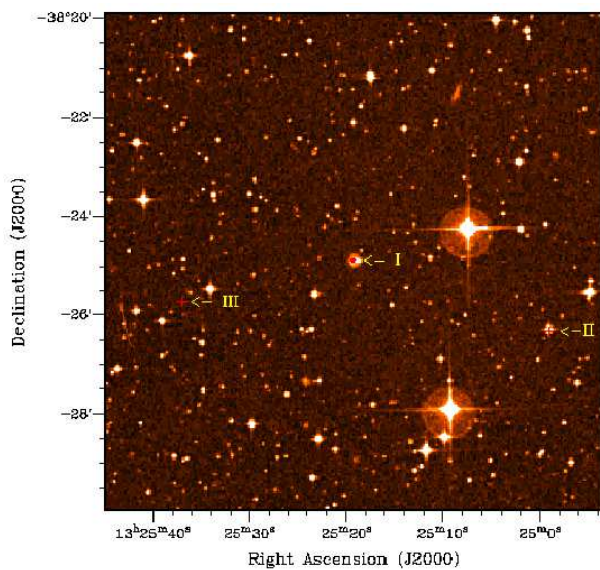


Fig. 1. Optical image (taken from DSS) overlaid with *CHANDRA* X-ray contour map of IRAS 13224–3809 and marked *CHANDRA* X-ray position of the sources GSC 7787 01660 (II) and RX J132537–3825 (III).

The *CHANDRA* X-ray positions of two other sources, GSC 7787 01660 (II) and RX J132537–3825 (III), are marked by a cross. Note that no optical counterpart is found in optical catalogues for the source RX J132537–3825 (III). For the source detection we have used CELLDETECT from the *CHANDRA* CIAO data analysis package. The centroid position for IRAS 13224–3809 in the *CHANDRA* image, computed with CELLDETECT, is $\alpha_{2000} = 13^{\text{h}}25^{\text{m}}19.41^{\text{s}}$, $\delta_{2000} = -38^{\circ}24'52.85''$. The coordinates of IRAS 13224–3809 and the two other X-ray sources are listed in table 1. Fig. 2 shows an higher resolution optical image with the *CHANDRA* position marked by a red cross. The agreement between the X-ray positions and optical positions obtained from the GSC catalogue is within 2 arcsec.

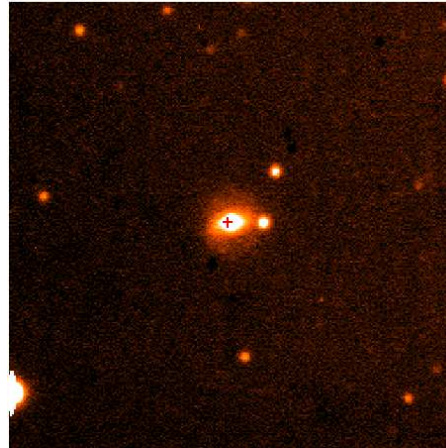


Fig. 2. *CHANDRA* X-ray position marked with red cross in a deeper optical image (subrange of Fig. 1) with higher resolution observed at the ESO-Danish 1.54m telescope.

4. Timing properties of IRAS 13224–3809

In this section we discuss the properties of the light curve of IRAS 13224–3809, including the indications for a quasi-periodic signal and the tests for periodicity.

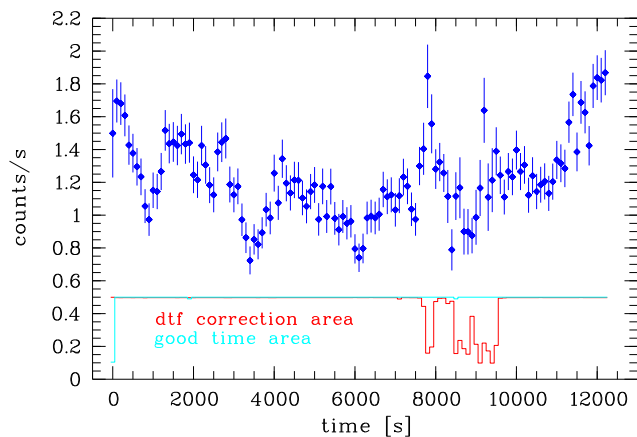


Fig. 3. Light curve of IRAS 13224–3809 combined with deadtime correction file (dtf) and goodtime correction file of the second processed data (correction files are shifted down by factor of $\frac{1}{2}$). Note the larger error in the 2000 sec region of dtf correction - for description see section 2.. The light curve indicate a quasi periodicity with a period of 2500 s.

In Fig. 3 we show the *CHANDRA* light curve of IRAS 13224–3809. The reason for the lack of flaring events compared to the *ROSAT* observations in 1996 (Boller et al. 1997) is probably due the short exposure time (12 ksec) of the observation. However, the light curve exhibits flux variations with the strongest flux change by a factor 2 within 600 sec. The efficiency calculation shows that the change of luminosity

Table 1. **Coordinates:** X-ray (using CELLDETECT) and optical coordinates (taken from HST GSC catalogue) of IRAS 13224–3809, GSC 7787 01660 (RX J132459–3826) and RX J132537–3825.

name		<i>CHANDRA</i> position			optical position			$\Delta\alpha$	$\Delta\delta$						
		α_{2000}		δ_{2000}	α_{2000}		δ_{2000}								
		[h]	[m]	[s]	[°]	[′]	[″]	[h]	[m]	[s]	[°]	[′]	[″]	[″]	[″]
IRAS 13224–3809	(I)	13	25	19.41	-38	24	52.85	13	25	19.28	-38	24	53.48	1.95	-0.63
GSC 7787 01660	(II)	13	24	59.20	-38	26	18.53	13	24	59.20	-38	26	17.18	0.0	1.35
RX J132537–3825	(III)	13	25	37.09	-38	25	42.66	-	-	-	-	-	-	-	-

over time ($\Delta L/\Delta t = 3.2 \cdot 10^{41} \text{ergs}^{-2}$) exceeds the maximum allowed value by accretion onto a Schwarzschild black hole. This fact points to the presence of a Kerr black hole in IRAS 13224–3809. The ‘peak emission’ of the light curve is not well defined and flattened, however four well-defined count rate minima are clearly visible and separated by 2500 sec. This fact and the shape of the count rate variations seems to be an indication for a quasi-periodic signal in IRAS 13224–3809. In Fig. 4, the light curve with an inverted count rate axis illustrates the sharp and clearly separated peaks at 900, 3400, 6000, 8700 and 10800 seconds.

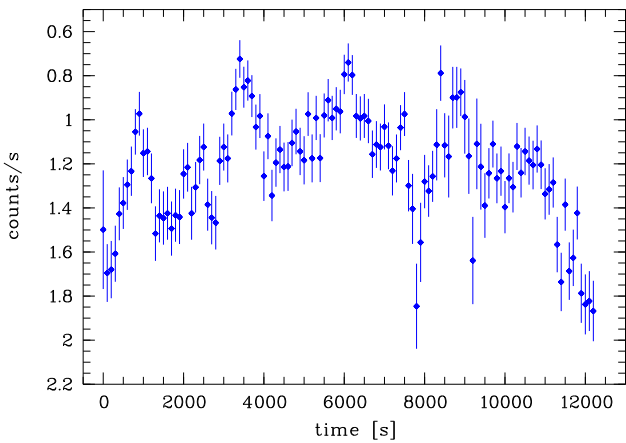


Fig. 4. Light curve with inverse count rate axis of IRAS 13224–3809 illustrate the sharp and clearly separated peaks. The light curve indicate a quasi periodicity with a period of 2500 s.

The mean count rate of IRAS 13224–3809, obtained from the light curve, is $\text{cps} = 1.222 \pm 0.010 \text{ counts s}^{-1}$. The unabsorbed flux in the 0.1 - 10.0 keV energy range computed with W3PIMMS¹ using a power law and black body model with the spectral parameters; hydrogen column density $N_{\text{H}} = (0.87 \pm 0.05) \cdot 10^{21} \text{cm}^{-2}$ (Boller et al., 1996), photon index $\Gamma = 2.47$, temperature $kT = 0.121 \text{ keV}$ (Brandt, private communication) and the relative normalisation $n = 0.2181$ at 1.0 keV; results in

*1 <http://heasarc.gsfc.nasa.gov/Tools/w3pimms.html>

$F_{\text{X}} = (4.310 \pm 0.035) \cdot 10^{-11} \text{erg cm}^{-2} \text{ s}^{-1}$ corresponding to the X-ray luminosity $L_{\text{X}} = (3.880 \pm 0.036) \cdot 10^{44} \text{erg s}^{-1}$ (for $z = 0.0667$, $q_0 = \frac{1}{2}$ and $H_0 = 75 \text{ km s}^{-1} \text{Mpc}^{-1}$).

4.2. Tests of periodicity - χ^2 , FFT, Lomb - Scargle

To probe the quasi-periodic oscillation we used four independent tests. In Fig. 5, the strongest signal in the Lomb-Scargle periodogram is 2500 sec. The second strong signal at 1300 sec seems to be the higher order of the signal at 2500 sec. The same result is given by the power spectrum of the source in Fig. 6.

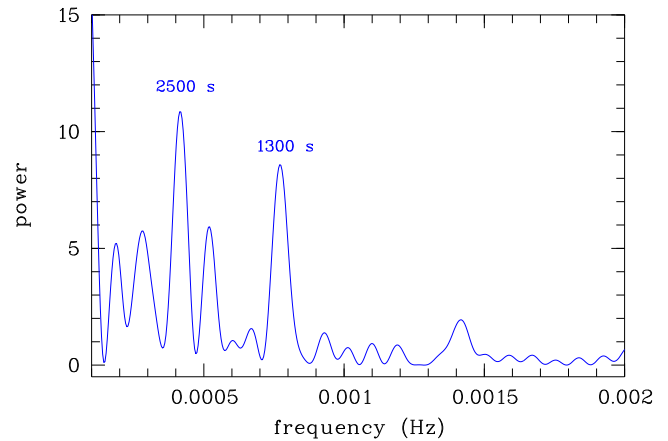


Fig. 5. Lomb scargle test for periodicity in the 0.2-10 keV energy range.

We have folded the light curve with different periods, ranging from 500 to 3500 seconds, and have determined the corresponding χ^2 value. The reduced χ^2 versus the folding period in Fig. 7 shows also the strongest peak at 2500 sec. The corresponding folded light curve is given in Fig. 8 with the best fitting period of 2400 sec and modulations of about 20 %. We made simulations of light curves with the observed time sequence and phase randomized for a red noise f^{-1} power spectrum (see Fig. 9). The indication for the periodic signal in the light curve of IRAS 13224–3809 (see the power spectrum in Fig. 6) are in the same order compared to the power

seen in the simulated power spectrum. Therefore we need the 80 ksec *XMM-Newton* observation of the source to confirm the presence of any quasi-periodic signal.

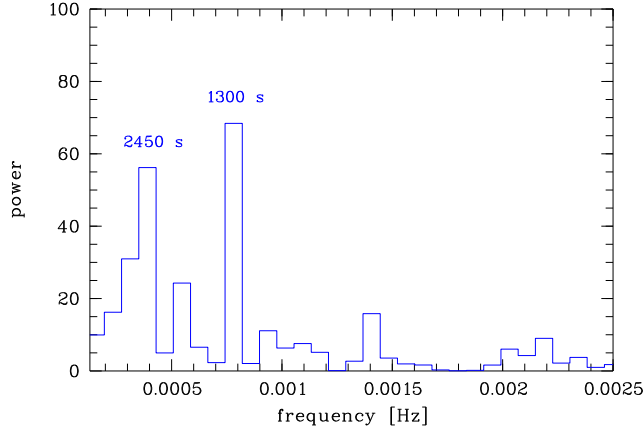


Fig. 6. Power spectrum for IRAS 13224–3809 in the 0.2–10 keV energy range.

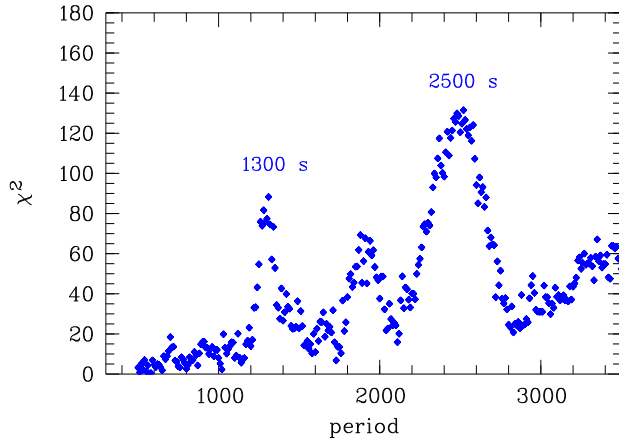


Fig. 7. Reduced χ^2 versus the folding period for the 0.2–10 keV energy range.

5. Discussion

The quasi-periodic oscillations if confirmed by other X-ray observations, can be caused by instabilities of the inner parts of the accretion disk, which can lead to variations of the accretion rate. In this case the period is expected to be of the order of the radial drift time scale (“instability time scale”)

$$\tau \sim \frac{\epsilon}{\alpha} \cdot \left(\frac{r}{R_S} \right)^{\frac{3}{2}} \cdot \frac{R_S}{c}$$

with $\epsilon \sim 5 - 10$ and $\alpha \sim 0.1$ (Sunyaev, private communication). For a period of 2500 sec and a mass of

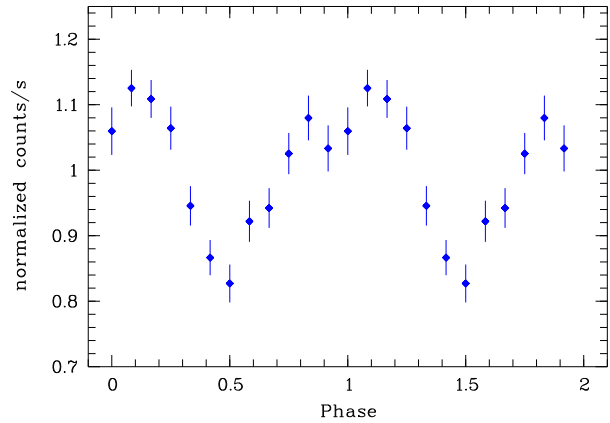


Fig. 8. The light curve of IRAS 13224–3809, folded with a period of 2380 s.

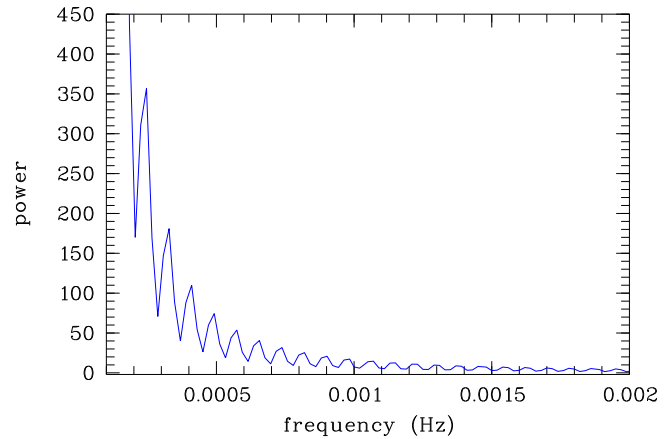


Fig. 9. Simulated red noise power spectrum of IRAS 13224–3809, normalized to the real data set.

$M_{\text{BH}}^{\text{Edd}} \sim 3 \cdot 10^6 M_{\odot}$ derived from the Eddington limit, we have estimated a radius of $r \approx 1.4 R_S$, where the instabilities occur, which would be also indicative for the presence of a Kerr black hole. Absorption by Compton-thick matter can probably be ruled out by an estimation for the distance of the absorbing matter.

In Fig. 10 we show the lower and upper value of the black hole mass for IRAS 13224–3809. The lower mass is given by the Eddington limit ($M_{\text{BH}}^{\text{lower}} \sim 3 \cdot 10^6 M_{\odot}$). The upper mass limit is estimated from material orbiting with $v = c$ ($M_{\text{BH}}^{\text{upper}} \sim 4 \cdot 10^7 M_{\odot}$). The blue curve demonstrates the dependence of black hole mass to different rotation radii in units of the Schwarzschild radius, assuming that rotating Compton-thick matter is causing the X-ray periodicity (semi-relativistic calculation)².

^{*2} $\frac{v}{c} = \sqrt{\frac{r}{2(r-1)^2 + r}}$; r in units of R_S and $v = \frac{2\pi \tilde{r}}{T}$; $\tilde{r} = r \cdot R_S$

The putative Compton-thick absorbing material has to be located at distances of $\sim 5 R_S$. This seems to be inconsistent with neutral Compton-thick absorbing material, because it is too close to the central black hole.

Boller Th., Brandt W.N., Fabian A.C., Fink H.H., 1997
MNRAS, 289, 393
Sunyaev R.A., 1973, Soviet Astron. AJ, 16, 941
Sunyaev R.A., 2000, private communication

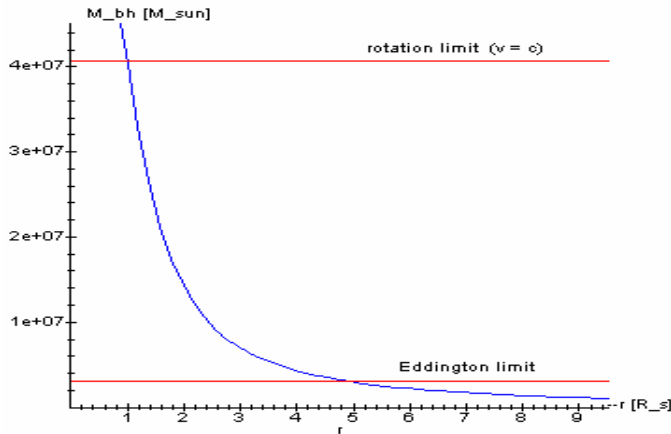


Fig. 10. Dependence of black hole mass to different rotation radii for rotating Compton-thick matter (blue curve). The radius is given in units of the Schwarzschild radius and the black hole mass in units of solar mass.

6. Summary

The precisely determined X-ray position of the flaring source IRAS 13224–3809 (Boller et al. 1997) is in good agreement with the optical position from the Hubble GSC of the galaxy (within 2 arcsec). The light curve of IRAS 13224–3809 shows no huge flaring events as seen by Boller et al. (1997); however, we found indications for a quasi-periodic signal in the light curve of IRAS 13224–3809 with a period of 2500 sec. This quasi-periodic signal might be caused by instabilities of inner parts of the accretion disk. To confirm and to study the triggering processes of the putative periodic signal we need the scheduled *XMM-Newton* observation which will yield both timing and spectral information of this source.

In addition, we found evidence for the presence of a Kerr black hole in IRAS 13224–3809. The first hint is given by the change of luminosity over time, which exceeds the maximum allowed value by accretion onto a Schwarzschild black hole. The second one is the estimation of the distance of the accretion disk instabilities to the black hole, resulting in the short distance of about 1.4 Schwarzschild radii. We estimate the black hole mass of IRAS 13224–3809 between $3 \cdot 10^6 M_\odot$ and $4 \cdot 10^7 M_\odot$.

References

Boller Th., Brandt W.N., Fink H., 1996 A&A, 305, 53